(A.3)

THE INFLUENCE OF HEAVY DOPING EFFECTS ON SILICON SOLAR CELL PERFORMANCE

M. WOLF

Department of Electrical Engineering, University of Pennsylvania, Philadelphia, PA 19104 (U.S.A.)

(Received August 25, 1985; accepted August 26, 1985)

Summary

Many modern crystalline silicon solar cells are highly doped in both the emitter and the so-called back-surface-field (BSF) structure. Auger recombination and band-gap narrowing thus take place in these regions with detrimental effects on cell performance. Through a design study is has been shown that these effects negate the benefits of the BSF structure if the latter contains a layer doped to a higher concentration than about 10^{17} cm^{-3}, and that the primary benefit of the BSF structure is to permit the use of a thinner base region rather than to provide higher efficiency. For the emitter, a high dopant surface concentration is seen to be beneficial when the surface recombination velocity is high. However, to realize the cell performance gains potentially available from reducing the surface recombination velocity and the saturation current contribution from the base requires a reduction of the emitter dopant surface concentration. Attempts to obtain more than 20% (AM 1.5) efficiency will require the almost complete elimination of heavy doping effects through reducing the impurity concentration in the emitter.

1. Introduction

All presently used preparative methods for crysalline silicon solar cells, for production as well as developmental purposes, result in some parts of the devices being "heavily doped". In addition, many design approaches for such cells deliberately introduce a heavily doped region, such as in the back-surface-field (BSF) cells [1-4]. As a consequence of the introduction of impurities to the levels commonly encountered, "heavy doping effects", *i.e.* Auger recombination and band-gap narrowing, are incurred in some parts of the active volume of these devices.

With the present emphasis on developing silicon solar cells of higher efficiency, *i.e.* in the 18-20% (AM 1.5) range in the near term and ultimately

0379-6787/86/$3.50

greater than 20%, questions arise as to whether heavy doping effects do not actually impose limitations on the achievable efficiencies and to what degree heavy doping can provide a beneficial design compromise. Although it has been stated earlier that heavy doping effects are generally detrimental to solar cell performances [3, 5–7] and that the application of BSF structures brings no benefit except perhaps in extremely thin devices [8], not much attention has been given to these facts in more general thinking about high efficiency solar cell designs. This may in part have been caused by the lack of parametric design studies specifically aimed at demonstrating the influence of heavy doping effects on solar cell performance. The purpose of this paper is to provide such information and to clearly indicate the performance limitations imposed by heavily doped sections of the front and base regions of solar cells, as well as the role which such sections can play in design compromise.

2. Methodology

There are generally two regions in solar cells of conventional design in which heavy doping effects are encountered. One of these is the BSF structure, which in its original version involved a relatively thin diffused or ion implanted layer with a drift field just below the contact-covered back surface of the cell. The version of the BSF structure more commonly encountered today, which is generated by aluminum alloying and silicon regrowth, includes a high/low junction somewhat further from the back surface, and a rather uniformly doped layer between this high/low junction and the ohmic contact. The second region with high doping is the "emitter", which is generally a diffused or ion implanted front region. This is characterized by an impurity concentration gradient from the 10^{15} to 10^{17} cm^{-3} range at the junction space charge region edge to a surface concentration in the 10^{19} to 10^{21} cm^{-3} range.

Questions relating to the performance impacts of heavy doping effects can be readily studied by the application of analytical simulation methods. Such methods are based on the analytical solution of the "Shockley equations" for carrier transport in semiconductors. These solutions are fully valid as long as the problem is one-dimensional and the superposition principle is applicable: this requires primarily that the low level injection condition is fulfilled. For the study of heavy doping effects, however, a simulation method is needed which is capable of handling layer structures. Such a solution is described in ref. 9, and is embodied in the program SPCOLAY for personal computers (program available from the author upon request) which has been used for the present study.

In addition to the usual analytical formulation of the performance of a solar cell as a function of its design parameters, a physical description of the heavy doping effects is also required. The data of Slotboom and de Graaff [10] have been used to describe the amount of band-gap narrowing

as function of impurity concentration, and this band-gap change has been applied in its entirety to the edge of the minority carrier band. This has implications for the drift fields to which the minority carriers are subjected. For the Auger recombination, the broadly accepted Auger coefficients as determined by Dziewior and Schmidt [11] have been used. Besides Auger recombination, the Shockley–Read–Hall recombination mechanism for deep traps has been used with the usual summation of the recombination rates. A Shockley–Read–Hall saturation lifetime of 1 ms was assumed. It should be noted that these assumptions have some influence on the results of this study, as a lower saturation lifetime would have a tendency to shift the efficiency maxima somewhat toward higher doping levels (as well as to lower efficiency values!). The assumption of a shallower trap level should have the effect of broadening the maxima. Use of the Kendall lifetime/doping relationship [12] in lieu of the Shockley–Read–Hall relationship (see ref. 3, fig. 6, curve labeled "Fischer–Pschunder") would have the same effect.

3. Influence of impurity concentration on the effect of α-BSF structure

Increasing the doping of the layer located between the high/low junction and the ohmic contact in the BSF structure will generally provide a higher potential barrier at the high/low junction. This will improve its effect of "shielding" the minority carriers in the less heavily doped part of the base region from the higher transport velocities which exist on the "high side" of the high/low junction. This approach could be used to reduce the influence of the high surface recombination velocity of the ohmic contact. However, if the thickness of the layer between the high/low junction and the ohmic contact is chosen to be of the order of the minority carrier diffusion length L within this layer, then this high side transport velocity u_{high} is essentially the bulk recombination velocity L/τ of this layer, rather than the surface recombination velocity. The bulk recombination velocity can generally be made substantially lower than the surface recombination velocity of a contact, so that the effect of this layer is to isolate the base from the effects of the ohmic contact. The transport velocity u is transformed across the high/low junction (effects of band-gap narrowing being excluded) according to the relation

$$\frac{u_{\mathrm{low}}}{u_{\mathrm{high}}} = \frac{N_{\mathrm{low}}}{N_{\mathrm{high}}} \tag{1}$$

where N_{low} and N_{high} represent the majority carrier concentrations on the sides of this junction that are less and more heavily doped respectively (see ref. 9, eqn. (9)). Thus, increasing N_{high} will generally lead to better "shielding". When, however, with increasing majority carrier concentration, Auger recombination bcomes dominant so that

$$\tau = (C_{\mathrm{Auger}} N_{\mathrm{high}}{}^2)^{-1} \tag{2}$$

the bulk recombination velocity will increase in proportion to this concentration

$$u_{\text{high}} = \left(\frac{D}{\tau}\right)^{1/2} = (D\,C_{\text{Auger}})^{1/2} N_{\text{high}} \tag{3}$$

with the result that the minority carrier transport velocity on the "low side" of the high/low junction will become essentially independent of the impurity concentration on the "high side"

$$u_{\text{low}} = N_{\text{low}} (D\,C_{\text{Auger}})^{1/2} \tag{4}$$

If band-gap narrowing is added on the more heavily doped side, then the effective barrier height of the high/low junction is decreased, and with it the transport velocity transformation ratio.

To quantify these effects, the efficiency of a solar cell has been calculated with all of its design parameters held constant except for the impurity concentration and the thickness of the highly doped layer (between the high/low junction and the ohmic contact) of the base. The thickness of the less heavily doped layer (located between the p/n junction and the high/low junction) of the base has been held at 200 μm, or about 1/6 of a diffusion length, and its acceptor concentration initially at $5 \times 10^{16}\,\text{cm}^{-3}$. The acceptor concentration of the heavily doped layer was varied from that of the less heavily doped layer up to $5 \times 10^{20}\,\text{cm}^{-3}$, with the minority carrier mobility and lifetime changed downward with increasing doping, the latter according to Shockley–Read–Hall and Auger recombination theory, starting from the lifetime value of 8×10^{-4} s at $5 \times 10^{16}\,\text{cm}^{-3}$ acceptors. In one group of data, the thickness of the highly doped layer was made equal to the diffusion length of the layer. Also, to separate the effects of Auger recombination from those of band-gap narrowing, the broken curve in Fig. 1 was obtained with Auger recombination as the only heavy doping effect.

For a more heavily doped layer of one diffusion length thickness, the efficiency was found to increase slightly from the value obtained for 5×10^{16} acceptors cm^{-3}, *i.e.* without a high/low junction, up to the acceptor density of $1 \times 10^{17}\,\text{cm}^{-3}$ in this layer, and then to decrease somewhat toward higher acceptor concentrations. If the layer is kept at a constant thickness of 1200 μm (equal to one diffusion length at 5×10^{16} acceptors cm^{-3}), independent of the acceptor concentration, then the efficiency increases a little more, up to a maximum at an acceptor density of $2 \times 10^{17}\,\text{cm}^{-3}$, after which it also falls off (continuous curve in Fig. 1). At an acceptor concentration of about $4 \times 10^{18}\,\text{cm}^{-3}$, the relative thickness (physical thickness divided by diffusion length) of the p^+ layer exceeds 36, leading to exponent overflow at still higher values. For this reason the thickness was held to ten diffusion lengths at acceptor densities above $4 \times 10^{18}\,\text{cm}^{-3}$. In this range the resulting continuous curve in Fig. 1 is seen to asymptotically approach the broken curve obtained for unit relative thickness. Considering band-gap narrowing in addition to Auger recombination, a much more dramatic fall-off of the

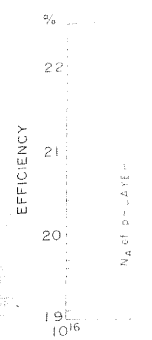

Fig. 1. Con
BSF structu
ness is 200
cated. The
includes ba
AM 1 solar

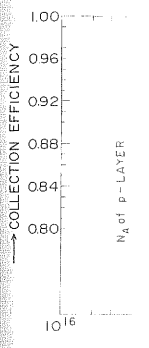

Fig. 2. Colle
p^+ layer acce

conversion
the p^+ laye
To b
influence
ency and
collection
efficiency.
density sh
height of
gap narro
recombina
current is
concentrat

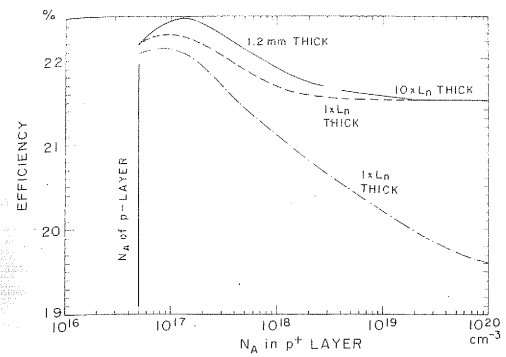

Fig. 1. Conversion efficiency as a function of acceptor concentration in the p^+ layer of a BSF structure, with all parameters outside the p^+ layer held constant. The p layer thickness is 200 μm, its acceptor concentration 5×10^{16} cm^{-3}. The p^+ layer thickness is indicated. The two upper curves are based on Auger recombination only; the lower curve also includes band-gap narrowing (Slotboom model). The efficiency data are based on the AM 1 solar spectrum.

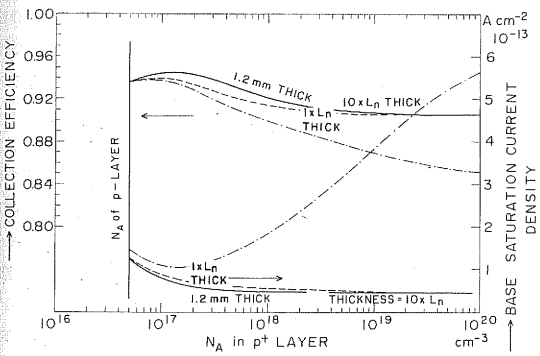

Fig. 2. Collection efficiency and base saturation current contribution as a function of the p^+ layer acceptor concentration for the cases presented in Fig. 1.

conversion efficiency is observed with increasing acceptor concentration in the p^+ layer (chain curve in Fig. 1).

To better demonstrate the underlying physics, Fig. 2 illustrates the influence of the acceptor concentration in the p^+ layer on collection efficiency and on the saturation current contribution of the base region. The collection efficiency curves follow the pattern seen in Fig. 1 for conversion efficiency. At relatively low acceptor concentrations the saturation current density shows the expected reduction resulting from the increasing barrier height of the high/low junction. After that, when computed without band-gap narrowing, it levels off due to the increasing dominance of Auger recombination. When band-gap narrowing is also considered, the saturation current is seen, in this range, to rise substantially with increasing acceptor concentration.

The foregoing discussions lead to the conclusion that a doping level which corresponds to the onset of the heavy doping effects is the most favorable one. But this conclusion should also apply to the less heavily doped base layer. This would mean that a uniformly doped base with 1×10^{17} acceptors cm^{-3} should be optimal. This postulate was investigated in a further study, in which the acceptor concentration of the less heavily doped base layer was also varied. When the total base thickness was held to 1400 μm (corresponding to the continuous curve of Fig. 1), the efficiencies reached with the uniformly doped bases did not approach that of the optimum high/low junction with the same base thickness. When the base thickness was made equal to one diffusion length in every case, the efficiency was even lower in most cases. However, when the base thickness was increased to three diffusion lengths, the efficiency in the case of an acceptor concentration of $1 \times 10^{17}\,cm^{-3}$ reached that obtained with the best high/low junction, which also had doping of $1 \times 10^{17}\,cm^{-3}$ in the more heavily doped layer. While the uniform concentration of $5 \times 10^{16}\,cm^{-3}$ showed a nearly equal efficiency, the efficiencies fell off more rapidly on approaching higher and lower acceptor concentrations than did those for the high/low junctions.

The findings outlined in the preceding paragraph lead to the conclusion that no absolute efficiency benefit can be derived from the use of a BSF structure (high/low junction with a "thick" more heavily doped layer). However, an equal maximum efficiency can be achieved with a thinner device structure when such a BSF system is used. This observation holds at least for the cases of large diffusion lengths which are of interest for very high efficiency devices. It has also been seen that for a uniformly doped base the acceptor concentration range 5×10^{16}–$1 \times 10^{17}\,cm^{-3}$ yields the highest efficiencies, while for the high/low junction designs a concentration of 2×10^{16}–$5 \times 10^{16}\,cm^{-3}$ acceptors in the less heavily doped layer and of 1×10^{17}–$2 \times 10^{17}\,cm^{-3}$ in the more heavily doped layer gives the best results.

4. Influence of heavy doping effects on performance of the front region

The front regions of silicon solar cells, whether obtained by diffusion or by ion implantation with subsequent activation annealing, contain a large impurity gradient between the edge of the space charge region of the p/n junction and the front surface. The impurity distribution in many devices approximates a complementary error function and in others a Gaussian or an exponential distribution. Considering layers of equal thickness and with the same surface concentration of the impurity, it can be seen that the average impurity concentration in the front region is lower for the exponential distribution than for the other two distributions. Thus, the influence of the heavy doping effects should be smallest for the exponential distribution. The computations discussed below were carried out using the exponential impurity distribution and should thus represent the least severe case for the influence of heavy doping effects on emitter performance. To verify this, a

control run with a complementary error function distribution was carried out using a surface concentration of $2 \times 10^{20}\,cm^{-3}$. This showed that the saturation current was hardly affected but that the collection efficiency was significantly reduced compared to that found using the exponential distribution.

The cell parameters used originally represented the structure of Westinghouse's 18.1% efficient silicon solar cell [13]. This includes a base region with a BSF structure, a dual-layer anti-reflection coating, a nominal junction depth of 0.3 μm and a donor concentration of $2 \times 10^{17}\,cm^{-3}$ at the front region edge of the p/n junction space charge region. Except for the donor distribution in the emitter and the parameters directly connected with it, all cell design parameters were kept invariant throughout the study. It was found that too many of the structures investigated were base limited, so that the results of the emitter doping study were obscured; for this reason the base was later replaced by a single layer of reduced total recombination. The data presented in Figs. 3 and 4 result from this latter base region.

The donor concentration at the surface of the emitter was varied by factors of ten from 2×10^{18} to $2 \times 10^{21}\,cm^{-3}$. The front region between the surface and the edge of the junction space charge region was divided into five layers, each 0.05 μm thick (except for the layer next to the p/n junction

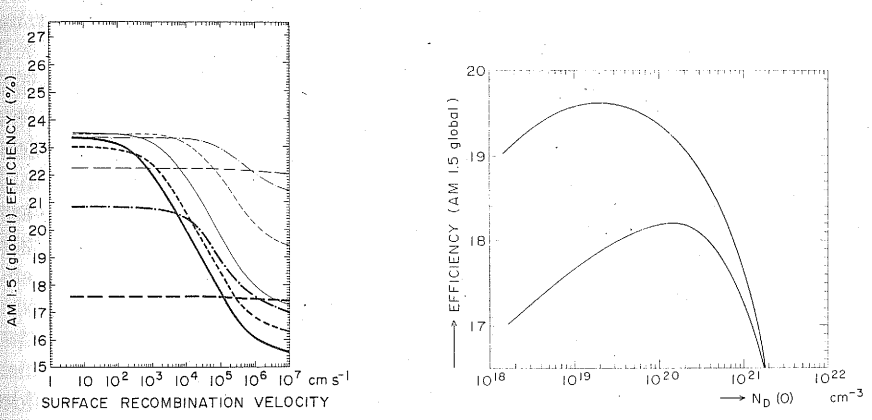

Fig. 3. Conversion efficiency as a function of the surface recombination velocity of an emitter with an exponential donor concentration and a nominal junction depth of 0.3 μm. The donor concentration at the junction space charge region edge was held constant (as a parameter) at $2 \times 10^{17}\,cm^{-3}$, while that at the surface varied as follows: ——, $2 \times 10^{18}\,cm\,s^{-1}$; ····, $2 \times 10^{19}\,cm\,s^{-1}$; -·-, $2 \times 10^{20}\,cm\,s^{-1}$; - - -, $2 \times 10^{21}\,cm\,s^{-1}$. Lighter lines reflect the contribution of Auger recombination only.

Fig. 4. Efficiency as a function of surface donor concentration for two cases of surface recombination velocity: $5 \times 10^{4}\,cm\,s^{-1}$ (lower curve) to represent an Si solar cell without special treatment and $5 \times 10^{3}\,cm\,s^{-1}$ (upper curve) to represent a cell with oxide surface passivation. Note that the primary efficiency gain from passivation is obtained after lowering the surface donor concentration by an order of magnitude from its optimum value for the untreated cell. Other parameters are the same as those in Fig. 3.

which was slightly thinner). The minority carrier mobilities and lifetimes were held constant within each layer. Their values were determined as appropriate for a donor concentration equal to the geometric mean of the concentrations existing at the two boundaries of each layer, using literature data for the mobility values [14]. The intrinsic carrier concentration in each layer, taking band-gap narrowing into account, was also calculated according to the geometric mean donor concentration.

It had been suspected that the beneficial effects of the drift field which results from the impurity gradient might outweigh the detrimental effects of the heavy doping for the cases with higher surface recombination velocities. Computations were therefore carried out to determine the conversion efficiency as a function of the surface recombination velocity, with the donor surface concentration as a parameter. The results show that with a donor surface concentration of $2 \times 10^{21}\,\mathrm{cm}^{-3}$ the efficiency is practically independent of the surface recombination velocity (Fig. 3). This means that the heavy doping effects completely dominate the performance of the emitter. Nevertheless, at the highest surface recombination velocity values studied ($>10^6$ cm s^{-1}), a front region with such a high donor concentration still provides the highest conversion efficiency. In the surface recombination velocity range 10^4–$10^6\,\mathrm{cm\,s}^{-1}$, a surface donor concentration of $2 \times 10^{20}\,\mathrm{cm}^{-3}$ yields the best efficiencies, while at lower surface recombination velocity values (300–$10\,000\,\mathrm{cm\,s}^{-1}$), a surface concentration of $2 \times 10^{19}\,\mathrm{cm}^{-3}$ is optimal. Further reductions in surface concentrations will be needed to realize the potential of still lower surface recombination rates.

Recent experiments with passivation of the front surface of silicon solar cells have shown that improvements in conversion efficiency could be obtained only when the passivation efforts were accompanied by a reduction in the donor surface concentration from the $10^{20}\,\mathrm{cm}^{-3}$ to the low $10^{19}\,\mathrm{cm}^{-3}$ range. Some of the data obtained from the BSF base region structure were therefore plotted in the form obtained by Rohatgi [13] and by Spitzer *et al.* [15] who have prepared samples with different donor surface concentrations both with and without surface passivation. Surface recombination velocity values of 5×10^4 and $5 \times 10^3\,\mathrm{cm\,s}^{-1}$ were used to represent the ranges of experimentally determined values on cells prepared without special attention to surface passivation and on cells provided with a thermal oxide respectively. The computed curves of Fig. 4 closely resemble those found experimentally. They show that a conversion efficiency gain of about one percentage point is obtainable by reducing the surface concentration simultaneously with the application of the thermal oxide.

The physical effects connected with the variation of the surface donor concentration primarily influence the saturation current contribution from the emitter. Figure 5 presents this contribution as a function of the surface recombination velocity, with the four values of donor surface concentration previously applied used as a parameter. All other device data are the same as those used for Fig. 3. As expected, for a donor surface concentration of $2 \times 10^{21}\,\mathrm{cm}^{-3}$ the saturation current density is high (about $6 \times 10^{-11}\,\mathrm{A\,cm}^{-2}$)

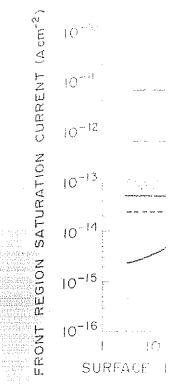

Fig. 5. Emit
velocity, with
Fig. 3. The h
magnitude e
surface recon

and indepe
tion provid
tion velocit
saturation
5×10^5 cm
$10^4\,\mathrm{cm\,s}^{-1}$.
concentrati
order of n
further dec
reduction i
tion velocit

For p
tion currer
region is r
reduced sti
in the surfa
and/or an
current co
concentrati
has made r
tion of the
ed to perm
velocity or
efficiencies
base regior
improving t
tion velocit

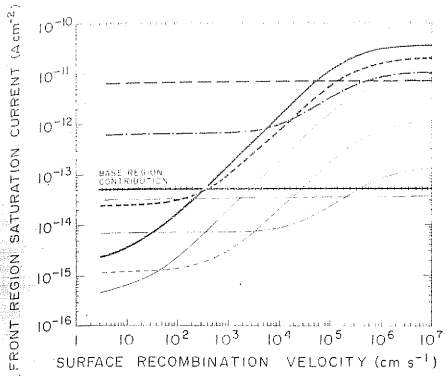

Fig. 5. Emitter saturation current contribution as a function of surface recombination velocity, with surface donor concentration as a parameter, for the cell design used for Fig. 3. The base region saturation current contribution is shown as a reference value: its magnitude explains the partial "efficiency saturation" observed in Fig. 3 for very low surface recombination velocity and surface donor concentration values.

and independent of the surface recombination velocity, but this concentration provides the lowest saturation current at the highest surface recombination velocity value. A surface concentration of $2 \times 10^{20}\,cm^{-3}$ provides lower saturation current densities at front surface recombination velocities below $5 \times 10^{5}\,cm\,s^{-1}$ and as much as a factor of ten lower for velocities below $10^{4}\,cm\,s^{-1}$. Below this value of surface recombination velocity, a surface concentration of $2 \times 10^{19}\,cm^{-3}$ yields lower saturation currents, with another order of magnitude reduction available for velocities below $10^{3}\,cm\,s^{-1}$. A further decrease of the surface concentration to $2 \times 10^{18}\,cm^{-3}$ provides a reduction in saturation current to below $10^{-14}\,A\,cm^{-2}$ at surface recombination velocities of less than 50 $cm\,s^{-1}$.

For purposes of comparison, the base region contribution to the saturation current has been entered as a cross-hatched line in Fig. 5. The base region is not optimal and its saturation current contribution might be reduced still further. Figure 5 leads to the clear conclusion that a reduction in the surface recombination velocity on the front surface to below $10^{4}\,cm\,s^{-1}$, and/or an improvement of the base region to provide a lower saturation current contribution would be without any effect if the donor surface concentration were held at or above $2 \times 10^{20}\,cm^{-3}$. A reduction to $2 \times 10^{19}\,cm^{-3}$ has made realizable the benefits of surface passivation, but a further reduction of the surface donor concentration to $2 \times 10^{18}\,cm^{-3}$ or less will be needed to permit the exploitation of further decreases of surface recombination velocity or of improvements in base region design. Aiming for projected efficiencies in silicon solar cells of above 20% will thus require improving base region design for a lower saturation current contribution, further improving the passivation of the front surface to below $10^{3}\,cm\,s^{-1}$ recombination velocity and abandoning the present practice of heavy doping near the

front surface of the device. The requirement for surface concentrations of $2 \times 10^{18}\,cm^{-3}$ or less may, in fact, eliminate the use of diffusion, or of ion implantation with subsequent activation annealing, as viable process options for the preparation of very high efficiency silicon solar cells.

5. Conclusions

Studies on the optimum impurity concentration in the more heavily doped layer of a BSF structure have clearly shown that any increase of the impurity concentration in this layer beyond the point where the band-gap narrowing effects start to exert an influence yields no performance gains. This point is reached at acceptor densities between 1×10^{17} and $2 \times 10^{17}\,cm^{-3}$. In fact, the same solar cell performance can also be obtained when the acceptor concentration in the entire base region is chosen in the 5×10^{16}–$2 \times 10^{17}\,cm^{-3}$ range, albeit with a greater base thickness. This leads to the conclusion that the use of a BSF structure in terrestrial cells will ultimately not provide any significant efficiency improvement but will permit the use of a smaller base thickness. For space cells, where radiation damage considerations often impose restrictions on the impurity concentration in the less heavily doped base layer, the use of the BSF structure can still increase efficiency, but designers should consider the results of this study. It should also be noted that these discussions have dealt only with the effects of the BSF structure on "shielding" and "isolating" the minority carriers from the effects of a high surface recombination velocity, but not with the effects on the contact resistance. Achieving a low contact resistance may require a heavily doped layer below the metal/semiconductor interface [16]; however, such a layer can be thin and can be considered as part of the ohmic contact itself.

Similarly, the high donor surface concentrations used in diffused or ion implanted emitters impose an upper limit on the performance obtainable with crystalline silicon solar cells. Efforts to reduce the surface recombination velocities on the emitter surface and to reduce recombination in and on the base region so as to lower its saturation current contribution will ultimately bear fruit and lead to over 20% (AM 1.5) efficient solar cells, only if they are accompanied by a reduction in doping of the emitter. Nevertheless, previous cell designs, with uncontrolled and very high front surface recombination velocities, were correct in using high surface concentrations on very thin emitters, as in this case the beneficial effect of the drift field obtained in the structure outweighed the detrimental influence of the heavy doping effects. A performance peak was thus reached which was, however, a compromise well below the theoretical performance level which should ultimately be attainable.

References

1 J. Mandelkorn and J. H. Lamneck, Jr., Simplified fabrication of back surface electric field silicon cells and novel characteristics of such cells, *Proc. 9th Photovoltaic Specialists' Conf., Pub. No. 72CH0613-OED*, IEEE, New York, 1972.

2 M. P. Godlewski, C. R. Baraona and H. W. Brandhorst, Jr., Low–high junction theory applied to solar cells, *Proc. 10th Photovoltaic Specialists' Conf., Palo Alto, CA, Nov. 1973, Pub. No 73CH0801-1*, IEEE, New York, 1973, p. 40.
3 D. L. Bowler and M. Wolf, *IEEE Trans. Components, Hybrids, Manuf. Technol., 3* (1980) 464.
4 J. A. Fossum, R. D. Nashby and S. C. Pao, *IEEE Trans. Electron Devices, 27* (1980) 785.
5 M. P. Godlewski, H. W. Brandhorst, Jr. and C. R. Baraona, Effects of high doping levels on silicon solar cell performance, *Proc. 11th Photovoltaic Specialists' Conf., Pub. No. 75CH0948-OED*, IEEE, New York, May 1975, pp. 32–35.
6 F. A. Lindholm, S. S. Li and C. T. Sah, Fundamental limitations imposed by high doping on the performance of pn junction silicon solar cells, *Proc. 11th Photovoltaic Specialists' Conf., Pub. No. 75CH0948-OED*, IEEE, New York, May 1975, pp. 3–12.
7 M. Wolf, *IEEE Trans. Electron Devices, 27* (1980) 751.
8 H. T. Weaver, *Sol. Cells, 5* (1982) 275.
9 M. Wolf, *IEEE Trans. Electron Devices, 28* (1981) 566.
10 J. W. Slotboom and H. C. de Graaff, *Solid State Electron., 19* (1976) 857.
11 J. Dziewior and W. Schmidt, *Appl. Phys. Lett., 31* (1977) 346.
12 D. Kendall, *Conf. on Physics and Applications of Li-Diffused Si*, NASA–Goddard, 1969.
13 A. Rohatgi, personal communication, 1984.
14 H. F. Wolf, *Semiconductors*, Wiley, New York, 1971, p. 276.
15 M. B. Spitzer, C. J. Keavney, S. P. Tobin, F. A. Lindholm and A. Neugroschel, Mechanisms limiting open circuit voltage in silicon solar cells, *Proc. 17th Photovoltaic Specialists' Conf., Orlando, FL, May 1984, Pub. No. 84CH2019-8*, IEEE, New York, 1984, pp. 1218–1224.
M. B. Spitzer, personal communication, 1984.
16 D. K. Schroeder and D. L. Meier, *IEEE Trans. Electron Devices, 31* (1984) 637.